The Rotational Zeeman Effect of 1,2,4-Trifluorobenzene

W. H. Stolze and D. H. Sutter

Abteilung Chemische Physik im Institut für Physikalische Chemie
der Christian-Albrechts-Universität zu Kiel

Z. Naturforsch. **44a**, 687–691 (1989); received May 11, 1989

Dedicated to Prof. Dr. H. D. Rudolph on the Occasion of his 65th Birthday

The rotational Zeeman effect of 1,2,4-trifluorobenzene has been studied for 8 low-J rotational transitions in magnetic fields between 1.9 and 2.4 Tesla. The observed susceptibility anisotropies and molecular g-values are: $(2\chi_{aa}-\chi_{bb}-\chi_{cc})=37.85(69)\cdot 10^{-6}$ erg G^{-2} mole^{-1}, $(2\chi_{bb}-\chi_{cc}-\chi_{aa})=56.85(54)\cdot 10^{-6}$ erg G^{-2} mole^{-1}, $g_{aa}=-0.0393(3)$, $g_{bb}=-0.0277(3)$, and $g_{cc}=0.0042(2)$. The Zeeman parameters have been used to derive the molecular electric quadrupole moments and vibronic ground state expectation values for the electronic second moments. The observed out-of-plane quadrupole moment is discussed with reference to an additivity scheme proposed earlier. The observed out-of-plane component of the molecular magnetic susceptibility tensor is in excellent agreement with the value predicted earlier from the CNDO/2-π-electron density alternation at the ring atoms.

Introduction

In the following we present a rotational Zeeman effect study of 1,2,4-trifluorobenzene. It forms part of a systematic investigation of substitution effects on the magnetic properties of fluorinated benzenes [1–5] and pyridines [4–6]. It was initiated to check a linear correlation postulated earlier to hold between the CNDO/2-electron charge density alternations at the ring atoms and the nonlocal π-electron contribution to the magnetic susceptibility perpendicular to the plane of the ring [4]. The latter serves as a quantitative criterion for the aromaticity of ring compounds with $(2n+2)$ π-electrons (compare Refs. cited in [4]).

Experimental

Eight low-J rotational transitions of 1,2,4-trifluorobenzene, whose microwave structure is shown in Fig. 1, were measured in the frequency range between 7 and 17 GHz. For the Zeeman measurements the waveguide absorption cells were placed in the gap of a high field electromagnet [6]. At the lower frequencies between 7 and 12.4 GHz we have used our standard Stark-effect modulated microwave spectrometer [7, 8] to record the spectra. Above 12.4 GHz we have used our superheterodyne bridge spectrometer [3, 9]. Phase stabilized Klystrons and, above 12.4 GHz, phase stabilized backward wave oscillators were used as radiation sources. In order to reduce collision broadening, sample pressure were kept below 0.9 Pa (6.8 mTorr) at cell temperatures close to 220 K. Typical experimental linewidths were 100 to 150 kHz full width at half height. Signal averaging of up to 256 digital frequency sweeps was used to achieve satisfactory signal to noise ratios.

Our new microcomputer based experiment control and data handling system is described in detail in [10]. Our observed zero field frequencies and Zeeman multiplets are listed in Table 1.

Analysis of the Zeeman Multiplets and Derived Molecular Parameters

For the analysis of the Zeeman spectra we have used the standard effective Hamiltonian of a rigid rotor molecule rotating in an exterior magnetic field (see Eqs. (III.11) and (III.12) of [11]). Because of the small molecular g-values and large magnetic susceptibility anisotropies which are typical for aromatic ring compounds (see Fig. 1.4 of [11]), the second order Zeeman effect dominates at fields close to 2 Tesla (20 kGauss) as used here. This leads to very asymmetric Zeeman patterns. As examples we present the Zee-

Reprint requests to Prof. Dr. D. H. Sutter, Institut für Physikalische Chemie, Universität Kiel, Olshausenstr. 40–60, D-2300 Kiel 1.

0932-0784 / 89 / 0700-0687 $ 01.30/0. – Please order a reprint rather than making your own copy.

Table 1. Zero field frequencies and rotational Zeeman splittings of 1,2,4-trifluorobenzene. Also given are the calculated splittings which follow from the optimized g-values and susceptibility anisotropies presented in Table 2. Magnetic field strengths are mean values averaged over the effective length of the absorption cell. For peaks from unresolved satellites the seventh column gives the intensity weighted means of the constituent satellites.

Rotational transition Unperturbed freq. ν_0 $J'K'_-K'_+ \leftarrow JK_-K_+$ Magn. field strength Selection rule	Observed splitting $(\nu_H-\nu_0)$ (kHz)	$M_{J'} \leftarrow M_J$		Rel. int.	Calculated splitting $(\nu_H-\nu_0)_{calc}$ (kHz)	Average of calc. spl. $(\nu_H-\nu_0)_{av}$ (kHz)	Difference obs.-av. (kHz)
2 2 0 ← 1 1 1							
10 582.850 MHz							
2.3595 Tesla	−328.	−1	−1	3	−344.	−344.	16.
$\Delta M=0$	169.	1	1	3	157.	157.	12.
	882.	0	0	4	870.	870.	12.
1.8836 Tesla	−1033.	−2	−1	12	−1038.	−1038.	5.
$\Delta M=1$	7.	−1	0	6	−6.	−6.	13.
	277.	2	1	12	266.	271.	6.
		0	−1	2	301.		
	909.	1	0	6	898.	898.	11.
2 2 1 ← 1 1 0							
10 155.682 MHz							
2.3592 Tesla	−645.	0	0	4	−629.	−629.	−15.
$\Delta M=0$	548.	1	1	3	507.	566.	−18.
		−1	−1	3	627.		
1.8840 Tesla	−268.	−2	−1	12	−264.	−264.	−4.
$\Delta M=1$	−57.	1	0	6	−49.	−46.	−11.
		0	1	2	−40.		
	491.	2	1	12	505.	505.	−14.
3 1 3 ← 2 0 2							
7 436.851 MHz							
1.8836 Tesla	−171.	−1	0	12	−184.	−179.	8.
$\Delta M=1$		0	−1	6	−169.		
	−26.	1	0	12	−21.	−21.	−5.
	109.	−2	−1	20	95.	109.	0.
		2	1	20	123.		
	264.	3	2	30	263.	263.	1.
	355.	−3	−2	30	369.	369.	−14.
3 1 2 ← 2 1 1							
7 072.739 MHz							
18858 Tesla	−376.	−1	0	12	−424.		
$\Delta M=1$		−2	−1	20	−391.	−387.	11.
		0	1	6	−301.		
	−200.	−3	−2	30	−200.	−200.	0.
	214.	1	0	12	149.		
		2	1	20	195.	212.	2.
		3	2	30	260.		
3 2 1 ← 2 1 2							
13 342.989 MHz							
2.3588 Tesla	−1184.	−2	−2	5	−1197.	−1197.	13.
$\Delta M=0$	182.	−1	−1	8	180.	180.	2.
	790.	1	1	8	749.	791.	−1.
		0	0	9	829.		
1.8890 Tesla	−1369.	−3	−2	30	−1368.	−1368.	−1.
$\Delta M=1$	−371.	−2	−1	20	−374.	−374.	3.
	234.	3	2	30	240.	240.	−6.
	811.	2	1	20	778.	804.	7.
		1	0	12	848.		
3 2 2 ← 3 1 3							
7 133.686 MHz							
2.3583 Tesla	−1658.	−3	−3	9	−1659.	−1659.	1.
$\Delta M=0$	−546.	−2	−2	4	−548.	−548.	2.
	−2.	3	3	9	−14.	−14.	12.
	548.	2	2	4	548.	548.	0.
4 2 2 ← 3 1 3							
16 549.101 MHz							
1.8886 Tesla	−1775.	−4	−3	56	−1759.	−1759.	−16.
$\Delta M=1$	−851.	−3	−2	42	−844.	−844.	−7.
	−155.	−2	−1	30	−184.		
		2	3	2	−88.	−157.	2.
		−1	−2	6	−43.		
	288.	−1	0	20	222.		
		1	2	6	270.	288.	0.
		4	3	56	313.		
	537.	0	−1	12	537.	537.	0.
	741.	3	2	42	751.	751.	−10.
4 2 3 ← 3 1 2							
13 577.554 MHz							
1.8886 Tesla	−347	−2	−1	30	−333.	−333.	−14.
$\Delta M=1$	−91.	−3	−2	42	−87.	−87.	−4.
	13.	1	0	20	14.	19.	−6.
		2	1	30	22.		
	116.	0	−1	12	112.	131.	−15.
		3	2	42	136.		
	242.	−4	−3	56	266.	266.	−24.
	341.	4	3	56	356.	356.	−15.

man multiplets of the $2\,2\,0 \leftarrow 1\,1\,1$ rotational transition observed under $\Delta M = 0$ and $\Delta M = \pm 1$ selection rule in Figure 2.

The three diagonal elements of the molecular g-tensor and the two linearly independent magnetic susceptibility anisotropies $(2\chi_{aa} - \chi_{bb} - \chi_{cc})$ and $(2\chi_{bb} - \chi_{cc} - \chi_{aa})$ were fitted to the total of 43 observed Zeeman splittings listed in Table 1. They are presented in Table 2. Two sets of g-values are compatible with the observed Zeeman splittings. The second set (II) however can be discarded since it would correspond to a negative value of the vibronic ground state expectation value for the out-of-plane second electronic moment $\langle 0 | \sum_i c_i^2 | 0 \rangle$ (see below).

For further analysis we have used these Zeeman parameters together with our rigid rotor rotational

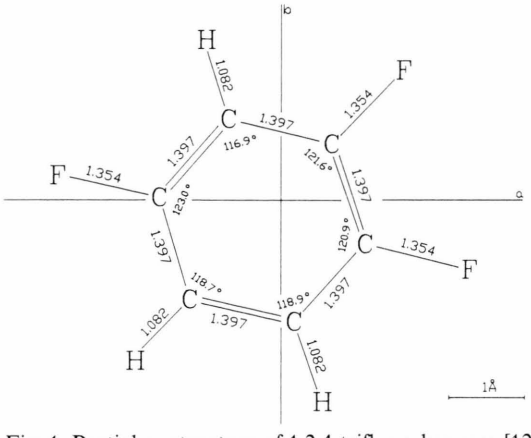

Fig. 1. Partial r_0-structure of 1,2,4-trifluorobenzene [12] also showing the orientation of the principal inertia axes system. The authors have accounted for deformations of the ring by substitution effects but they had to use the simplifying assumption that the peripheral bonds bisect the respective endocyclic angles. This structure was used to calculate the second moments of the nuclear charge distribution.

Table 2. g-Tensor elements and anisotropies in the diagonal elements of the molecular magnetic susceptibility tensor of 1,2,4-trifluorobenzene. Two sets of g-values, which only differ in sign, are compatible with the observed splittings. Set (II) can be discarded, however, since it would lead to an unreasonable negative value for the out-of-plane second electronic moment (see text). Uncertainties are single standard deviations of the least squares fit to the observed splittings.

	I	II
g_{aa}	−0.0393(3)	0.0393
g_{bb}	−0.0277(3)	0.0277
g_{cc}	0.0042(2)	−0.0042
$2\chi_{aa} - \chi_{bb} - \chi_{cc}$	37.85(69)	$37.85 \cdot 10^{-6}$ erg G^{-2} mole^{-1}
$2\chi_{bb} - \chi_{cc} - \chi_{aa}$	56.85(54)	$56.85 \cdot 10^{-6}$ erg G^{-2} mole^{-1}

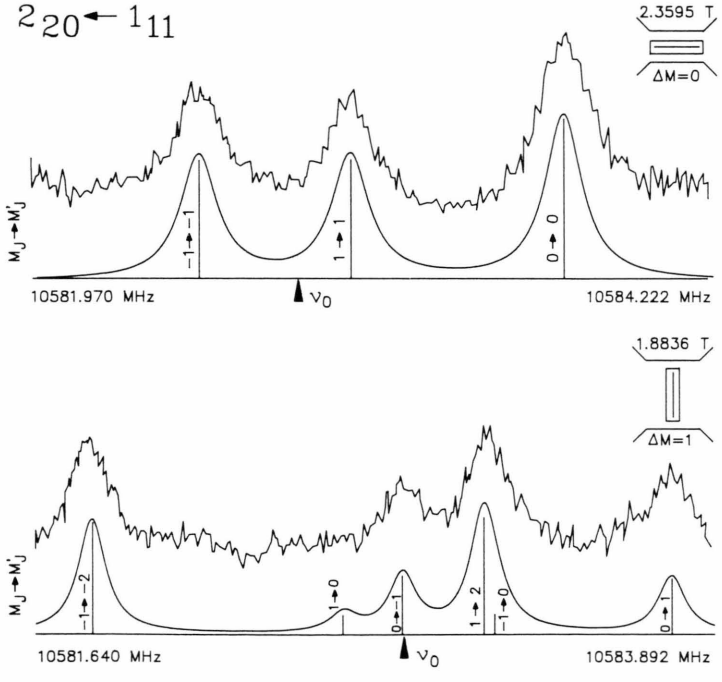

Fig. 2. Recordings of the Zeeman patterns of the $2\,2\,0 \leftarrow 1\,1\,1$ rotational transition observed under $\Delta M = 0$ (upper trace) and $\Delta M = \pm 1$ selection rule (lower trace). The computer simulations were calculated from the optimized g-values and susceptibility anisotropies (Table 2) under the assumption of Lorentzian lineshapes with full widths at half height of 150 kHz and 110 kHz, respectively. The insert shows the orientation of the waveguide cross section in the gap of the magnet. (The electric vector of the incident microwave radiation is polarized perpendicular with respect to the broad face of the waveguide.)

Table 3. Additional input data and derived molecular parameters of 1,2,4-trifluorobenzene. The rigid rotor rotational constants result from a least squares fit to our observed zero field frequencies. Given uncertainties are single standard deviations from least squares fits to experimental data (rotational constants and bulk susceptibility) or follow from experimental uncertainties by Gaussian error propagation (quadrupole moments etc.).

Rotational constants		
A	3083.997(2)	MHz
B	1278.360(1)	MHz
C	903.697(1)	MHz
Bulk susceptibility		
$1/3(\chi_{aa}+\chi_{bb}+\chi_{cc})$	−70.2(10)	10^{-6} erg G^{-2} mole^{-1}
Second moments of the nuclear charge distribution		
$\sum Z_n a_n^2$	191.82(10)	Å^2
$\sum Z_n b_n^2$	87.86(19)	Å^2
$\sum Z_n c_n^2$	0.00(00)	Å^2
Molecular electric quadrupole moments		
Q_{aa}	−11.21(114)	10^{-26} esu cm^2
Q_{bb}	10.27(120)	10^{-26} esu cm^2
Q_{cc}	0.94(162)	10^{-26} esu cm^2
Molecular magnetic susceptibilities		
χ_{aa}	−57.58(123)	10^{-6} erg G^{-2} mole^{-1}
χ_{bb}	−51.21(118)	10^{-6} erg G^{-2} mole^{-1}
χ_{cc}	−101.77(141)	10^{-6} erg G^{-2} mole^{-1}
Second moments of the electronic charge distribution		
$\langle 0 \mid \sum a_i^2 \mid 0 \rangle$	204.1(9)	Å^2
$\langle 0 \mid \sum b_i^2 \mid 0 \rangle$	97.2(9)	Å^2
$\langle 0 \mid \sum c_i^2 \mid 0 \rangle$	10.6(9)	Å^2 *

* Calculation with set II of Table 2 gives −9.0(9) Å^2.

Table 4. Local and nonlocal contributions to the in-plane ($(\chi_{aa}+\chi_{bb})/2$) and out-of-plane (χ_{cc}) susceptibilities of 1,2,4-trifluorobenzene. The value for the π-electron density alternation and the local atom increments for the susceptibilities were taken from [4].

	$(\chi_{aa}+\chi_{bb})/2$	χ_{cc}	
Experimental	−54.4	−101.8	10^{-6} erg G^{-2} mole^{-1}
local, calc.	−49.1	− 65.8	10^{-6} erg G^{-2} mole^{-1}
nonlocal	− 5.3	− 36.0	10^{-6} erg G^{-1} mole^{-1}

CNDO/2-π-density-alternation: 0.458.

constants to calculate approximate vibronic ground state expectation values for the molecular quadrupole moments (see chap. I.B of [11]) according to

$$Q_{aa} = \frac{|e|}{2}\left(\sum_{n}^{\text{nuclei}} Z_n(2a_n^2 - b_n^2 - c_n^2) - \langle 0 | \sum_{i}^{\text{electrons}} 2a_i^2 - b_i^2 - c_i^2 \mid 0\rangle\right)$$
$$= -\frac{\hbar\,|e|}{8\pi M}\left\{\frac{2g_{aa}}{A} - \frac{g_{bb}}{B} - \frac{g_{cc}}{C}\right\} - \frac{2mc^2}{|e|\,N}\{2\chi_{aa} - \chi_{bb} - \chi_{cc}\}. \quad (1)$$

The symbols have the following meaning: M = proton mass, m = electron mass, e = electron charge, c = velocity of light (the cgs-system is used throughout), N = Avogadro's number, $\hbar$ = Planck's constant divided by 2π, Z_n = atomic number of n-th nucleus, a_n = a-coordinate of n-th nucleus, a_i = a-coordinate of i-th electron etc.

With the second moments of the nuclear charge distribution calculated from the microwave r_0-structure [12] and with the liquid phase bulk susceptibility measured recently with the Faraday-balance method by Böttcher [13], we are also in the position to present the individual values for the diagonal elements of the magnetic susceptibility tensor as well as for the second moments of the electronic charge distribution. The latter were calculated according to

$$\langle | a^2 | \rangle = \langle 0 | \sum_{i}^{\text{electrons}} a_i^2 \mid 0\rangle = \sum_{n}^{\text{nuclei}} Z_n a_n^2 - \frac{\hbar}{8\pi M}\left(\frac{g_{bb}}{B} + \frac{g_{cc}}{C} - \frac{g_{aa}}{A}\right) - \frac{2mc^2}{e^2 N}(\chi_{bb} + \chi_{cc} - \chi_{aa}). \quad (2)$$

As was already the case with the quadrupole moments they closely correspond to vibronic ground state expectation values.

In Table 3 we present these additional input data together with our derived molecular quantities. Note that all values presented here are referred to the molecular principal inertia axes system of 1,2,4-trifluorobenzene.

Discussion

We will first have a look at the molecular electric quadrupole moment. As outlined earlier in [4] (Figs. 5 to 7), a linear relation appears to hold between the out-of-plane component of the molecular quadrupole

moment and the number of fluorine substituents at the ring, n_F. Since for molecules with nonzero electrical dipole moment the molecular quadrupole moment depends on the choice of the coordinate system, the center of the aromatic ring was used as the common point of reference for this comparison. The relation which transforms the experimental Q_{cc} value into this common reference system (compare [11], p. 102) is given by

$$Q_{\perp} = Q_{cc} + \Delta a\, \mu_a + \Delta b\, \mu_{bb} . \quad (3)$$

Here $\Delta a = -0.27$ Å and $\Delta b = -0.29$ Å are the coordinates of the center of the ring with respect to the molecular principal inertia axes system of 1,2,4-trifluorobenzene, and $\mu_a = -0.884(10)$ D and $\mu_b = -1.088(4)$ D [14] are the experimental values for the components of its molecular electric dipole moment. The result, $Q_{\perp} = +1.49(162) \cdot 10^{-26}$ esu cm^2 nicely matches the least squares straight line through the experimental values in Fig. 7 of [4] at $n_F = 3$. (The comparatively large uncertainty reflects the sensitivity of the derived Q_{cc} value with respect to minor uncertainties in the experimental g-values and susceptibility anisotropies.)

Second we will consider the nonlocal (i.e. π-ring current) contribution to the out-of-plane component of the magnetic susceptibility tensor, χ_{cc}.

Flygare and coworkers have proposed this value as a clear-cut quantitative criterion for "aromaticity" [15]. It is calculated as the difference between the experimental out-of-plane susceptibility minus the sum of the corresponding local atom susceptibilities. For 1,2,4-trifluorobenzene these local contributions to χ_{cc} add up to $\chi_{cc}^{\text{local}} = -65.79 \cdot 10^{-6}$ erg G^{-2} mole^{-2} (see [4], Table 5). Together with our experimental value listed in Table 3 this leads to $\chi_{cc}^{\text{nonlocal}} = -36.0 \cdot 10^{-6}$ erg G^{-1} mole^{-1}.

As mentioned already, Hübner, Stolze, and Sutter have presented evidence for a linear correlation between this nonlocal out-of-plane susceptibility and the CNDO/2-π-density alternation at the ring atoms (compare p. 340 of [4]). Using this linear correlation and the CNDO/2-π-density alternation of 0.458 (see Table 8 of [4]) Hübner et al. have predicted the nonlocal out-of-plane susceptibility of 1,2,4-trifluorobenzene as $-36.6 \cdot 10^{-6}$ erg G^{-2} mole^{-1} (compare Fig. 4 of [4]). This is in quite satisfactory agreement with our observed value of $-36.0 \cdot 10^{-6}$ erg G^{-2} mole^{-1}. We are therefore confident that the linear correlation will also be valid for the prediction of the magnetic susceptibility anisotropies in other hitherto unmeasured molecules of the substituted benzene and pyridine families.

Acknowledgements

The financial support by Deutsche Forschungsgemeinschaft and by Fonds der Chemischen Industrie Deutschlands is gratefully acknowledged. We would also like to thank Prof. Dr. A. Guarnieri for critically reading the manuscript. The computer calculations necessary to analyze the spectra were carried out at the DEC 10 system of the Rechenzentrum der Universität Kiel.

[1] D. H. Sutter, Z. Naturforsch. **29a,** 786 (1974).
[2] W. Czieslik, J. Wiese, and D. H. Sutter, Z. Naturforsch. **31a,** 1210 (1976).
[3] W. H. Stolze, M. Stolze, D. Hübner, and D. H. Sutter, Z. Naturforsch. **37a,** 1165 (1982).
[4] D. Hübner, M. Stolze, and D. H. Sutter, Z. Naturforsch. **36a,** 332 (1981).
[5] D. Hübner, M. Stolze, and D. H. Sutter, Z. Naturforsch. **37a,** 95 (1982).
[6] D. H. Sutter, Z. Naturforsch. **26a,** 1644 (1971).
[7] H. D. Rudolph, Z. Angew. Physik **13,** 401 (1961).
[8] U. Andresen and H. Dreizler, Z. Angew. Physik **30,** 207 (1970).
[9] M. Stolze, D. Hübner, and D. H. Sutter, J. Mol. Struct. **97,** 243 (1983).
[10] W. H. Stolze, Ph.D. thesis, Universität Kiel 1988.
[11] D. H. Sutter and W. H. Flygare, Top. Current Chem. **63,** 89 (1976).
[12] S. Doraiswamy and S. D. Sharma, J. Mol. Struct. **102,** 81 (1983).
[13] O. Böttcher, Diplom thesis, Universität Kiel 1986.
[14] J. Spieckerman and D. H. Sutter, Z. Naturforsch. **40a,** 864 (1985).
[15] T. G. Schmalz, C. L. Norris, and W. H. Flygare, J. Amer. Chem. Soc. **95,** 7961 (1973).